

Investigation of austenitizing temperature on wear behavior of austempered gray iron (AGI)

T. Sarkar¹, G. Sutradhara²

¹ Research scholar, School of Automotive Engineering, Jadavpur University, Kolkata

² Professor, Department of Mechanical Engineering, Jadavpur University, Kolkata

E. Mail: tannybesu@gmail.com

Abstract. This study is about finding the effect of austenitizing temperature on microstructure and wear behavior of copper alloyed austempered gray iron (AGI), and then comparing it with an as-cast (solidified) state. Tensile and wear tests specimens are prepared from as-cast gray iron material, and austenitized at different temperatures and then austempered at a fixed austempering temperature. Resulting microstructures are characterized through optical microscopy, scanning electron microscope (SEM) and X-Ray diffraction. Wear test is carried out using a block-on-roller multi-tribotester with sliding speed of 1.86 m/sec. In this investigation, wear behavior of all these austempered materials are determined and co-related with the microstructure. Hence the wear surface under scanning electron microscope showed that wear occurred mainly due to adhesion and delamination under dry sliding condition. The test results indicate that the austenitizing temperature has remarkable effect on resultant microstructure and wear behavior of austempered materials. Wear behavior is also found to be dependent on the hardness, tensile strength, austenite content and carbon content in austenite. It is shown that coarse ausferrite microstructure exhibited higher wear depth than fine ausferrite microstructure.

Keywords: *Austempered gray iron (AGI), Austenitizing temperature, Microstructure, Mechanical properties, Alloyed*

1. Introduction

Gray cast iron is a versatile material due to its very good castability, low-cost, high machinability and wear resistance properties which leads to specific and large use gray iron in today's era including past few decades also [1-3]. Gears, pinions, crankshafts are the most common parts for application of gray iron. Cylinder linear and similar type of parts which requires high wear resistance is also application area of gray iron and it brings interest in wear behaviour of gray cast iron [2, 3]. Austempered heat treatment process is applied on gray cast iron to produce austempered gray iron (AGI), development of ausferrite (ferrite and high carbon and stable austenite) microstructure so that properties can be improved [4]. Austempered gray iron (AGI) becomes an important structure material in recent years due to its outstanding mechanical properties. Among outstanding mechanical properties there are high hardness, strength with good ductility and good wear resistance. Due to excellent properties of AGI have also



various applications of structural components of industry and automobile sector such as gears, piston, locomotive wheel and agricultural equipment etc. [5-6].

Austempering process is an isothermal heat treatment process (austempering), which involves austenitizing in the temperature range of 871°C to 982°C (1600°F-1800°F) and then immediate quenching is done which leads it to an intermediate temperature range of 260°C to 385°C (500°F-725°F) and holding for sufficient time [7]. During the austempering of gray cast iron, variation in microstructures is observed which is dependent on the heat treatment parameters i.e. austenitising and austempering time and temperature respectively [5, 8]. Due to Austempering treatment, a matrix of bainitic ferrite or ausferrite structure is formed. Carbon-enriched austenite also an outcome during austempering treatment which leads to better combination of mechanical and wear resistance properties in comparison to as-cast (solidified) state [9-11]. From rigorous literature survey, it is found that some works are there on the influence of the heat treatment parameters (austenitizing, austempering temperature) of the microstructure on the mechanical and wear properties of AGI [3-13]. However, the research work on the wear properties of AGI is not so much in line of its application. The effect of its microstructure on tribological behavior for various working conditions and the mechanisms behind wear has still not been fully explored. Therefore, scope of the present investigation is based on the study of wear behavior of copper alloyed AGI for different austenitizing temperatures and to study the influence of microstructure on wear depth.

2. Experimental procedure

Blocks of gray cast iron keel with a chemical composition in wt%: 3.46C; 2.27Si; 0.53Mn; 0.5Cu; 0.19P; 0.1S ; (Table 1) are produced in a commercial gray iron foundry using cupola furnace. After melting, molten metal is poured into a standard 30 mm Y block sand molds (ASTM A-395) at temperature 1490°C, which is able to produce perfect castings. Tensile specimens with 6.35 mm diameter and 31.75 mm gauge length (Figure 1) as per ASTM E-8 standards [14] and wear test samples of suitable size (20x20x8 mm) (Figure 2) are machined from Y blocks respectively. The austempering process is schematically shown in Figure 3 (a, b). In austempering process, the specimens are first austenitized at different temperatures such as 871°C (1600°F), 898°C (1650°F), 927°C (1700°F), 954°C (1750°F) and 982°C (1800°F) for 1 h and then it is rapidly transferred to a salt bath (53%KNO₃, 40%NaNO₂ and 7%NaNO₃) at a constant austempering temperatures 310 °C (590°F), held for 1h and then air-cooled in room temperature to obtain distinctive microstructures. Table 2 is show the mechanical and wear properties of as-cast and austempered gray iron (AGI).

For microstructural characterization, standard metallographic preparation techniques (mechanical grinding and polishing followed by 2% Nital etching) are applied prior to characterization through optical microscope (Leica) and scanning electron microscope (SEM, JSM 6360). X-Ray diffraction (XRD) analysis is performed to calculate the relative proportions of volume fraction of austenite, following the procedure described by Dasgupta et al. [15]. It is done through X-Ray diffractometer (Rigaku, Ultimal III) instrument using monochromatic copper Fe-K α radiation (1.54059Å) at 40 kV and 30 mA. The scanning angular (2θ) ranged from 30° to 90° at a scanning speed of 1°/min. The profiles are analyzed using Jade 7 software to obtain peak positions and integrated intensities of (111), (220) and (311) planes of FCC austenite and (110), (200) and (211) planes of BCC ferrite. In addition, the percentage of carbon content in austenite (C_γ) is calculated using the equation $C_\gamma = (\alpha_\gamma - 3.548)/0.044$. Where α_γ is the lattice parameter calculated from the angular position of austenite peak [16]. The hardness of the samples is determined using Brinell hardness tester carried out under a load of 750 kg with 5mm ball and a dwell time of 10 seconds. The tensile tests are carried out at room temperature as per ASTM-E8 Standard [14] with a crosshead speed of 1 mm/min using a computerized Instron-8801 electromechanical testing machine. The tensile strength and percentage of elongation values are calculated. The as-cast and austempered wear specimens are tested in block-on-roller mechanism using a standard Ducom made multi-tribotester with

the linear speed 1.86m/sec and a 75 N load is applied on samples at room temperature. The roller disc is made up of hardened EN31 steel with surface hardness of 62 HRC. The worn surfaces of the wear test specimens are also examined using scanning electron microscope (SEM) which has operated at 20 kV. Four specimens are tested for each heat treatment and the average values are taken.

Table 1. Chemical composition of gray cast iron (wt %)

Materials	C	Si	Mn	Cu	P	S
Gray Iron (CG 20)	3.46	2.27	0.53	0.50	0.19	0.1

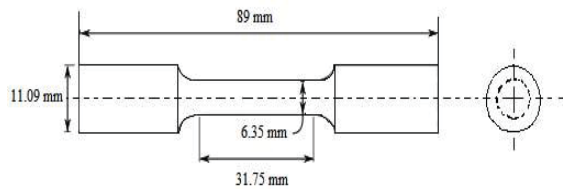


Figure 1. Schematic of machined tensile bar (ASTM-E8)

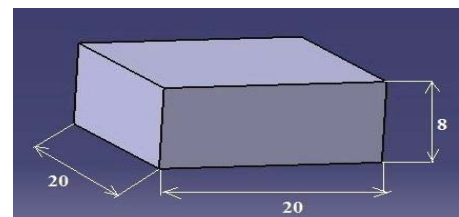


Figure 2. Schematic of wear test specimen (20X20X8 mm)

Table 2. Mechanical and wear properties of as-cast and austempered gray iron (AGI)

Samples condition Austempering temperature (°C)	Hardness (BHN)	Strength (MPa)	Elongation (%)	Wear (µm)
871-310	321	302	0.712	34
898-310	332	309	0.72	44
927-310	324	298	0.716	46
954-310	314	293	0.712	54
982-310	302	284	0.695	62
As-cast	209	172	0.6352	174

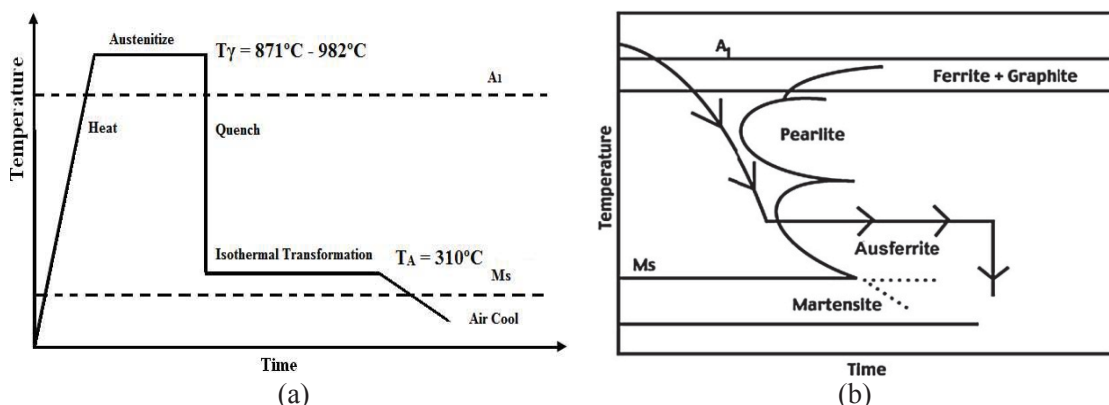


Figure 3 (a, b). Austempering process diagram

3. Results and discussions

3.1. Microstructure and phase analysis

The microstructures of the as-cast gray iron material are shown in Figure 4 (a, b). It is obvious from this microstructure that an upper mostly pearlitic matrix including dispersed graphite flakes is present. The presence of enormous graphite flakes serves as stress raiser, hence transmitting brittleness to the metal. Figure 5 (a–e) and 6 (a–e) shown the variations in the austempered microstructures. Where dark etching part is needle shaped of bainitic ferrite and the bright etching austenite with graphite flakes is dispersed. Simultaneously, changing of fine ferrite needles to coarser ferrite needles is observed in connection with increase of austenitizing temperature. From microstructure it is also obvious that the volume fraction of austenite increases with the increase of austenitizing temperature from 871°C (1600°F) to 982°C (1800°F). Systematic variation in the microstructure is seen that at lower austenitizing temperature more dark areas of ferrite are observed whereas at higher austenitizing temperatures more bright areas of austenite are identified. Thus, increasing the austenitizing temperature resulted in coarsening of the ferrite, as well as an increase in the volume fraction of austenite.

The optical and SEM microscopy are able to give a qualitative picture of the microstructural evolution but to get quantitative information there is a need of the X-ray diffraction technique. This is well supported by the X-ray diffraction analysis (Figure 7) where the relative amounts of austenite and carbon content in austenite are estimated at different austenitizing temperatures. Figure 8 reports the effect of austenitizing temperature on the volume fraction of austenite in the matrix. It is observed that the volume fraction of the austenite increased from 10.2 to 13.5% as the austenitizing temperature is increased from 871°C to 982°C. It is evident that volume fraction of austenite increase with increasing austenitizing temperature. At higher austenitizing temperature less ferrite is nucleated, consequently the matrix contains more austenite [17]. At this temperature the austenite becomes steadier and it influences the amount of ferrite in the matrix by decreasing amount. In Figure 9, the carbon content of austenite has been plotted against austenitizing temperature. It is evident shows that the carbon content of austenite increases with increasing austenitizing temperature. It is observed that the carbon content increased from 1.73 to 1.775 % as the austenitizing temperature is increased from 871°C to 982°C. Moreover, it is evident that the volume fraction of austenite and carbon content in austenite has similar trends with the austenitizing temperature.

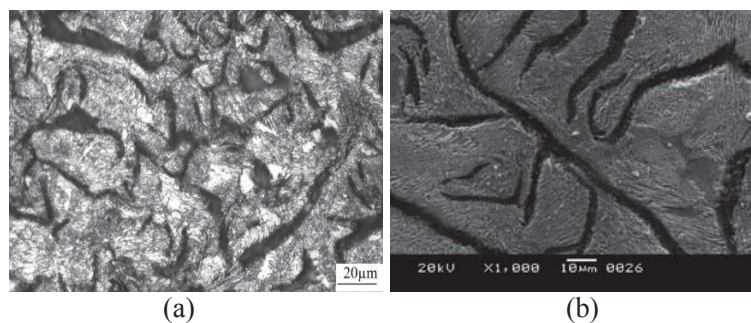


Figure 4. Micrographs of an as-cast gray iron (a) Optical Microstructure (500X) (b) SEM Microstructure

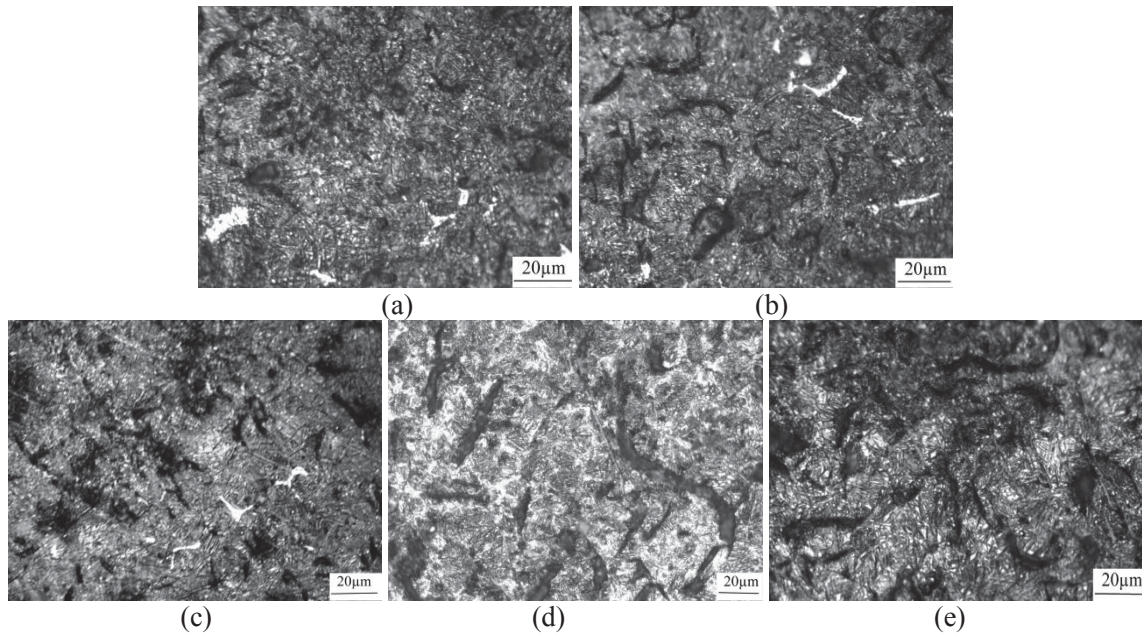


Figure 5. Optical micrographs (500X) of AGI samples (a) austenitized at 871°C (1600°F) for 1 h. (b) austenitized at 898°C (1650°F) for 1 h. (c) austenitized at 927°C (1700°F) for 1 h. (d) austenitized at 954°C (1750°F) for 1 h. (e) austenitized at 982°C (1800°F) for 1 h.

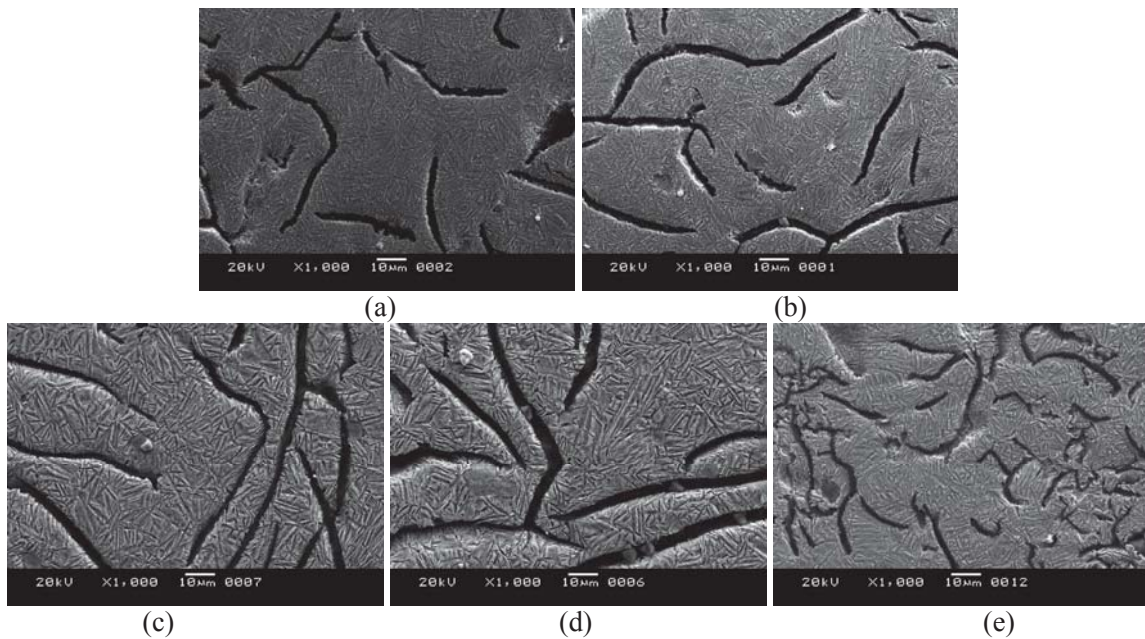


Figure 6. SEM micrographs of AGI samples (a) austenitized at 871°C (1600°F) for 1 h. (b) austenitized at 898°C (1650°F) for 1 h. (c) austenitized at 927°C (1700°F) for 1 h. (d) austenitized at 954°C (1750°F) for 1 h. (e) austenitized at 982°C (1800°F) for 1 h.

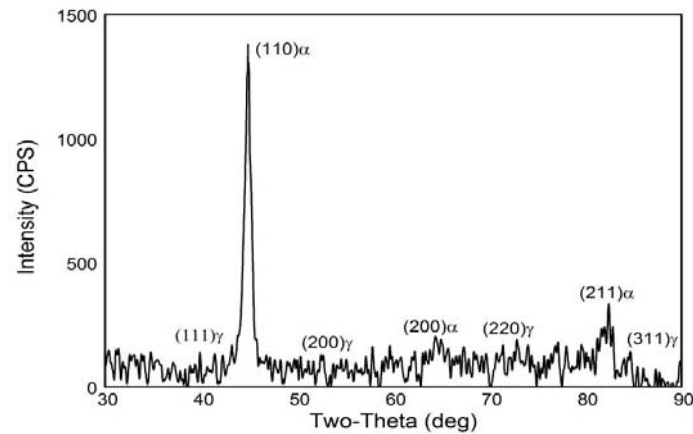


Figure 7. XRD phase analysis, austenitized at 927°C (1700°F) for 1 h.

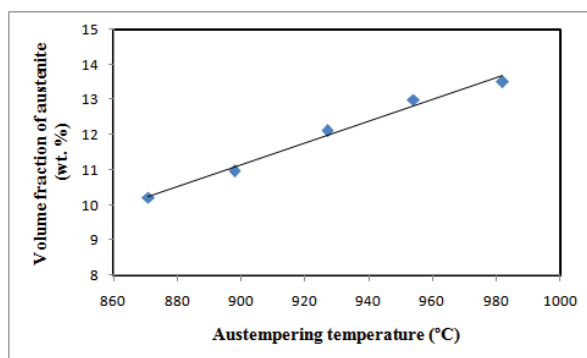


Figure 8. Effect of austenitizing temperature on volume fraction of austenite

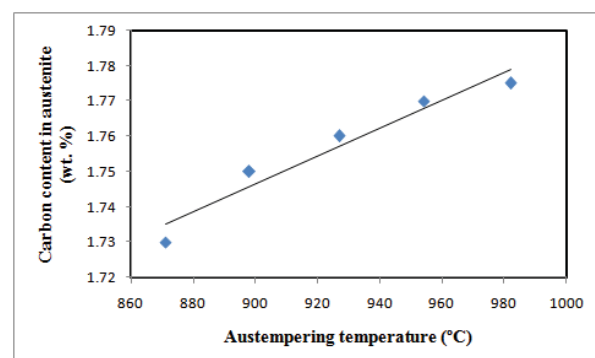


Figure 9. Effect of austenitizing temperature on the carbon content of austenite

3.2. Mechanical properties

The change of hardness and tensile strength with different austenitizing temperatures are shown in Figure 10 and 11. The report indicates initially increase and gradually decrease in hardness, tensile strength as the austenitizing temperature is increased. During austempering process, low hardness and tensile strength has obtained at higher austenitizing temperature and higher hardness and tensile strength obtained at lower austenitizing temperature. The microstructure appearance coarser at high austenitizing temperature and it leads to reduction in hardness as well as tensile strength. As the austenitizing temperature increases, volume fraction of austenite will increase, therefore a linear relationship is obvious from the XRD phase analysis indicates that volume fraction of austenite increases when hardness and tensile strength decreases. The sample austenitized at 871°C exhibited a hardness of 321 BHN and tensile strength of 302 MPa. But hardness and tensile strength decreases to 302 BHN and 284 MPa respectively, when austenitizing temperature comes into 982°C. In case of as-cast state, the values of hardness and tensile strength are lesser than austempered materials. Comparison of as-cast mechanical properties with properties after austempering is given in Table 2. The effect of elongation as a function of austenitizing temperatures are shown in Figure 12. However, ductility also decreases from 0.712% at 871°C to 0.695% at 982°C. It is evident that lower values of elongation are obtained at higher austenitizing temperature and vice versa. It

is also shown that elongation is initially increasing and gradually decreasing with the increase of austenitizing temperatures due to coarsening of matrix microstructure [17]. This type of behaviour is not prominent in as-cast state. Lee et al. [18], reported similar observation as stated above.

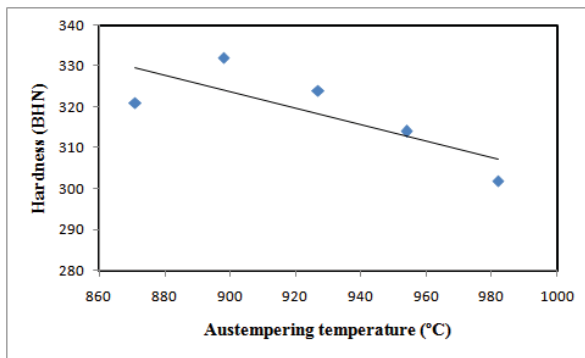


Figure 10. Effect of austenitizing temperature on hardness (BHN)

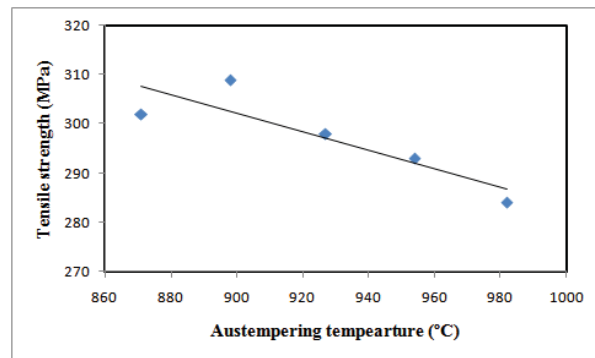


Figure 11. Effect of austenitizing temperature on tensile strength (MPa)

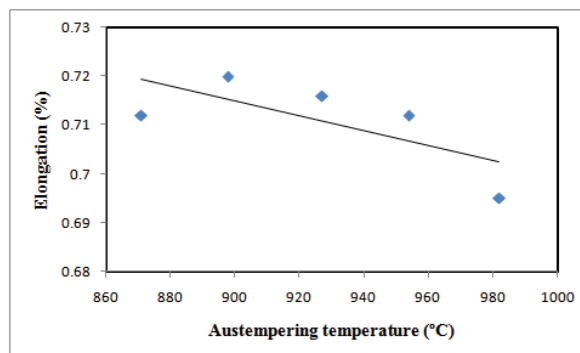


Figure 12. Effect of austenitizing temperature on Elongation (%)

3.3. Wear study

In the present study, the wear occurred due to the contact between a moving surface and a fixed surface. Moving surface is created by a hardened roller steel disc and the fixed one is a “block-of-sample” which is pressed against the moving disc with a constant load. Plastic flow of the materials is probably the main reason behind mechanism of wear and the direction of plastic flow is on the direction of rotation of block of samples surface. Due to generation of temperature and plastic flow of materials adhesion between two contacting surfaces may be happened which results tear of the samples surface and it is also a phenomenon behind wear mechanism. Oxidation of iron samples is common out come so iron oxide, which is brittle in nature can easily worn out from the samples surface and can gouge out the material [19]. Austenitizing temperature, hardness, tensile strength and austenite content, all of these have an effect on wear behavior of the prepared samples which is shown in Figure 13. It is obvious from the samples austenitizing at 871°C contains minimum wear depth and these increases with increase of austenitizing temperature. At lower austenitizing temperature like 871°C-898°C, closely spaced of fine sheaves of ferrite and austenite are observed together. This leads to high hardness and tensile strength, which also leads to excellent wear resistance properties. But at higher austenitizing temperatures such as 927°C and above, coarsen and

feathery ferrite with austenite is observed. This microstructure leads to less hardness and tensile strength [17], as well as wear resistance.

Figure 14 and 15 (a-e) shows the SEM studies of the worn surfaces are carried out to understand the nature of the wear process. Figure 14, SEM evidence of as-cast wear test material, where high plastic flow and tongue formation occur and void of graphite pull-out and its dragging to worn surface can found. The SEM images direct that at lower austenitizing temperatures such as 871°C-898°C, the wear surface initially consist of plastic flow and shallow wear scars with small pits as shown in Figure 15 (a, b). As the austenitizing temperature is increased the surface appearance changed markedly to show signs of scuffing and microcracks. With further rise in temperature (e.g 927°C and above), there are evidence of high plastic flow and tongue formation as shown in Figure 15 (c-e). Adhesion and delamination is the probable dominant phenomena. From this study, it can be concluded that as the austenitizing temperature increases, the volume fraction of austenite and carbon content in austenite also increase, simultaneously the wear resistance becoming less. The wear behavior is inversely proportional to the hardness, tensile strength. These parameters (like hardness, tensile strength and austenite content) act separately in influencing the wear resistance.

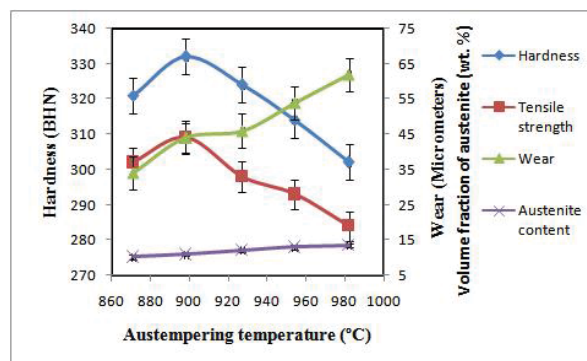


Figure 13. Effect of austenitizing temperature, hardness, tensile strength and austenite content on wear (μm)

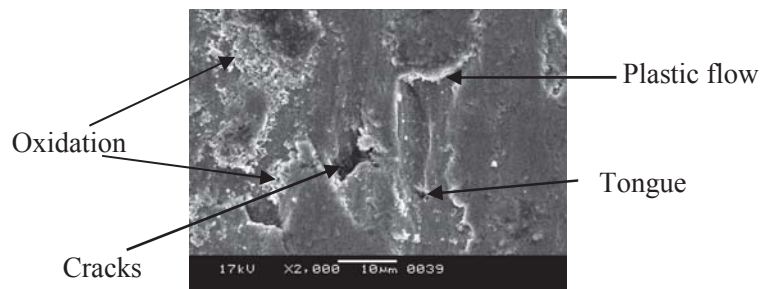


Figure 14. Worn surface of SEM micrographs of as-cast specimen

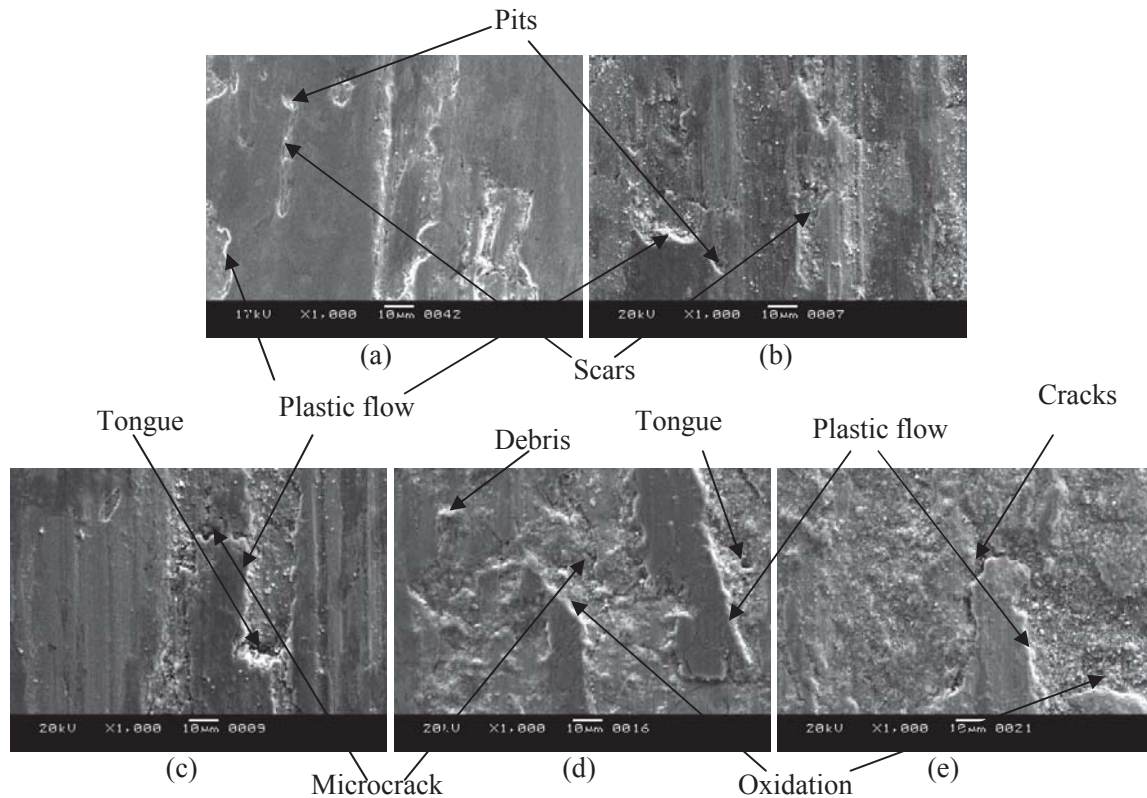


Figure 15. Worn surface of SEM micrographs of AGI samples (a) as-cast specimen (b) austenitized at 871°C (1600°F) for 1 h. (c) austenitized at 898°C (1650°F) for 1 h. (d) austenitized at 927°C (1700°F) for 1 h. (e) austenitized at 954°C (1750°F) for 1 h. (f) austenitized at 982°C (1800°F) for 1 h.

4. Conclusions

From the present investigation of copper alloyed AGI, following conclusions can be drawn:

1. The volume fraction of austenite and carbon content in austenite increases with increasing austenitizing temperature.
2. The hardness and tensile strength decreases as the austenitizing temperature increases, due to excessive coarsen microstructure as well as volume fraction of austenite increase at higher temperature. Also the ductility decreases with the austenitizing temperature increases.
3. Wear depth increases with increasing austenitizing temperature, where as wear behavior is also dependent on the hardness, tensile strength as well as volume fraction of austenite and carbon content in austenite.
4. The optimum combination of austempering processing parameters is 898°C austenitizing temperature, 310°C austempering temperature and 1h of austempering time. At this combination of temperature and time, the maximum mechanical properties are obtained; i.e. hardness 332 BHN, UTS 309 MPa, elongation 0.72% and wear 44µm.

Acknowledgments

The authors are grateful to Binay Udyog Pvt. Ltd, Howrah for supplying the grey iron material and UGC authority for providing this work under Rajiv Gandhi National Fellowship (RGNF).

References

- [1] Khanna O P 2011 *Foundry Technology* (New Delhi: Dhanpath Rai Publishers)
- [2] Angus H T 1976 *Cast iron: physical and engineering properties* (London: Butterworth)
- [3] Collini L, Nicoletto G and Kone R 2007 *Mater. Sci. Eng. A.* **488** 529
- [4] Xu W, Ferry M and Wang Y 2004 *Mater. Sci. Eng. A.* **390** 326
- [5] Kovacs B V and Keough J R 1993 *AFS Trans.* **101** 283
- [6] Hsu C H, Shy Y H, Yu Y H and Lee S C 2000 *Mater. Chem. Phys.* **63** 75
- [7] Brandenberg K, Hayrynen K L and Keough J R 2001 *Gear Tech.* **18** 42
- [8] Rundman K B, Parolini J R and Moore D J **2005 AFS Trans.** **145 (5)** 1
- [9] Vadiraj A, Balachandran G and Kamaraj M 2010 *J. Mater. Eng. Perf.* **19** 976
- [10] Olawale J O, Olusegun K M, Ezemenaka D I and Adisa S B 2014 *CAMSR* **1** 17
- [11] Vadiraj A, Balachandran G, Kamaraj M and Kazuya E 2011 *Mater. Design* **32** 2438
- [12] Vadiraj A, Balachandran G, Kamaraj M B, Gopalakrishna K and Rao P 2010 *Mater Design* **31** 951
- [13] Vadiraj A, Balachandran G, Kamaraj M, Gopalakrishna B and Rao D V 2010 *Tribol Int* **43** 647
- [14] ASTM E-8 1992 *Annual Book of ASTM Standards*, vol. 03.01 p 545
- [15] Dasgupta R K, Mondal D K and Chakrabarti A K 2013 *Metall. Mater. Trans. A.* **44A** 1376
- [16] Bayati H and Elliott R 1995 *Mater. Sci. Techn.* **11** 118
- [17] Patatunda S K and Gadicherla P.K 1999 *Mater. Sci. Eng. A.* **268** 15
- [18] Lee S C, Lee C C 1988 *AFS Trans.* **96** 827
- [19] Kumari U R and Rao P P 2009 *J. Mater. Sci.* **44** 1082